Efficient Modeling of Floating Wind Arrays Including Current Loads and Seabed Bathymetry

Preprint

Matthew Hall, William West, Stein Housner, and Ericka Lozon

National Renewable Energy Laboratory

NREL is a national laboratory of the U.S. Department of Energy
Office of Energy Efficiency & Renewable Energy
Operated by the Alliance for Sustainable Energy, LLC

This report is available at no cost from the National Renewable Energy Laboratory (NREL) at www.nrel.gov/publications.

Contract No. DE-AC36-08GO28308

Conference Paper
NREL/CP-5000-87475
January 2024

Efficient Modeling of Floating Wind Arrays Including Current Loads and Seabed Bathymetry

Preprint

Matthew Hall, William West, Stein Housner,
and Ericka Lozon

National Renewable Energy Laboratory

NOTICE

EFFICIENT MODELING OF FLOATING WIND ARRAYS INCLUDING CURRENT LOADS AND SEABED BATHYMETRY

Matthew Hall*, William West, Stein Housner, Ericka Lozon

National Renewable Energy Laboratory
15013 Denver West Parkway, Golden, CO 80401 USA

ABSTRACT

Capabilities for modeling the effects of seabed bathymetry and current drag loads on a floating wind farm are now available in an open-source model for quasi-static analysis. In this model, mooring lines and dynamic cables are represented by a quasi-static solver that can quickly represent complex mooring/cabling arrangements and arrays of floating bodies. To account for seabed bathymetry, we expand the model to include a surface mesh that captures changes in water depth over a rectangular grid. We formulate modifications to the catenary equations that capture a mooring line's profile and tensions when contacting a slope seabed. To account for current drag loads on mooring lines and dynamic cables, we formulate a novel technique that rotates the reference frame so that the vector sum of the the weight and the current force are used in the catenary equations, while accounting for the seabed orientation. To complete the system, current drag loads on floating substructures are handled by inclusion of strip-theory drag calculations.

These new capabilities are verified by comparing with results from the established offshore dynamics models MoorDyn and OrcaFlex in equivalent steady-state scenarios. The results show very good agreement for both sloped seabeds and current loads. With computation times of the quasi-static model typically under one second, the model additions are a useful capability toward rapidly evaluating a floating wind array's response to environmental loads under realistic site conditions.

Keywords: Floating wind turbine, mooring system, current, drag force, seabed slope, bathymetry

1. INTRODUCTION

Developing floating wind farm designs under realistic site conditions requires evaluating different design possibilities while considering local metocean and seabed conditions. At early design stages, computationally efficient models are needed to rapidly explore the extensive set of design variables of a floating wind farm, such as the array layout, mooring systems, and dynamic power cables. The National Renewable Energy Laboratory is developing an integrated low-fidelity floating wind array model for this purpose. This paper presents the addition of two important components to the model: seabed bathymetry, and current drag loads on the floating platforms, mooring lines, and dynamic power cables.

Non-uniform seabed conditions have long been considered in mooring modeling, although the capability is typically not supported in simpler models. One of the first papers about modeling mooring lines on sloped seabeds is from Stanton et al. [1]. They adapted the catenary equations to support sloped seabeds and verified the model using field data from a drilling vessel. A variety of recent works discuss modified modeling methods that can support non-level seabeds [2–5]. These methods are typically using higher fidelity models that modify and extend the seabed boundary condition of the code to be at variable water depths and to consider slope. The existing physics can then work as normal except with altered boundary conditions.

There are also examples of modeling seabed slope in simpler quasi-static models, although these models are generally not made available. Roy and Banik implemented a quasi-static model with seabed slope in the commercial code ANSYS AQWA [6]. Batista and Perkovic developed simplified analytical solutions for mooring lines interacting with a uniformly sloped seabed [7], although the formulation does not account for line axial stiffness or seabed friction (which are standard features in other quasi-static models, such as those in the floating wind turbine simulator FAST [8, 9]). Chai et al. developed a more generalized quasi-static model that includes seabed slope along with the ability to have multiple segments to handle discontinuities in the seabed surface [10]. This latter example appears suitable for a variety of scenarios, but it has not been released for widespread use. There is still a need for general seabed bathymetry support in coupled, open-source models.

Another phenomenon that is important for floating systems but often not considered in simpler models is drag forces from

---
*Corresponding author: matthew.hall@nrel.gov

current. The effect of current drag forces on a floating substructure can be calculated simply by adding a force based on drag coefficients, but it is not so straightforward for the effects on mooring lines or dynamic power cables. Quasi-static models used for mooring or cabling systems typically assume a planar, catenary-curve solution based on a uniform distributed weight in each section. There is not a natural way to impose additional forces without disrupting the catenary formulation. The closest attempt in the literature is from Trubat et al. [11], with a method to account for the dynamic loads on a mooring line through the use of the catenary equations. They modified the apparent weight of the mooring line to also approximate the hydrodynamic forces acting on the line in the vertical direction. This does not provide an obvious solution for modeling current drag forces, as current velocities are primarily in the horizontal direction.

In this paper, we present a modeling approach that accounts for both seabed bathymetry and current drag forces in a quasi-static floating system model. Drag forces on the floating substructure are modeled using strip theory. For the more challenging phenomenon of current drag on mooring lines and power cables, we formulate a method that uses a rotational transformation to add a distributed current drag force to the weight vector along each line section, allowing the catenary equations to still be used. This approach requires that the model also support sloped-seabed scenarios, because when rotating the reference frame, the seabed becomes rotated also. Therefore, we also extend the catenary solution for cases in which the line rests on a sloped seabed, including line axial stiffness and seabed friction.

Put together, these capabilities allow quasi-static modeling of floating systems in situations with realistic bathymetric variations and the presence of sea currents. Section 2 of this paper presents the formulations for mooring lines on sloped seabeds, current loads on mooring lines and dynamic cables, and current loads on floating substructures. Section 3 presents results that demonstrate these capabilities and verify their accuracy by comparing against results produced from the dynamic models MoorDyn and OrcaFlex. Section 4 summarizes conclusions on these new model capabilities and how they fit in the larger effort to improve computationally efficient modeling of floating wind arrays.

2. METHODOLOGY

The modeling methods presented in this paper are housed within a low-fidelity floating array modeling framework that combines quasi-static and frequency-domain analyses. In this framework, each floating wind turbine units is handled by RAFT [12], which stands for Response Amplitudes of Floating Turbines, an open-source model that computes the static and frequency-domain dynamic responses of floating platforms and attached wind or tidal turbines. RAFT models a floating platform as an assembly of linear members that can have cylindrical or rectangular cross sections. A strip theory approach can then be used to estimate the hydrodynamic forces on each member.

The effects of mooring lines and dynamic cables are represented by MoorPy [13], a quasi-static mooring model that can quickly model complex mooring/cabling arrangements and arrays of floating bodies. MoorPy fits as a submodel within RAFT.

The combined model has typical computation times in the order of several seconds for evaluating a floating wind array's mean offsets and several minutes for evaluating its dynamic responses.

The new formulations for seabed bathymetry and current loads within MoorPy and RAFT are divided into the following three subsections: seabed slope, current loads on moorings/cables, and current loads on the substructure.
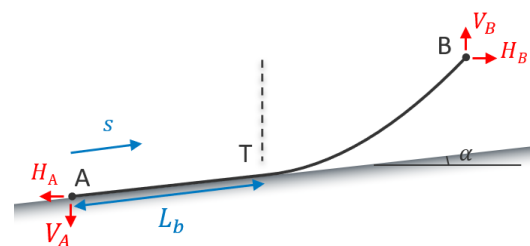
2.1 Mooring Lines on a Sloped Seabed

To account for seabed bathymetry, the MoorPy model has been expanded to replace the formerly flat seabed with a three-dimensional surface mesh that provides bathymetry over a rectangular grid. The computed profile for a given mooring line now accounts for the local seabed slope as defined by the grid. The standard mooring line catenary equations have been modified to describe the mooring line profiles and tension distributions when contacting a sloped seabed. This implementation is also applied to dynamic power cables, with the caveat that bending stiffness is neglected.

MoorPy's quasi-static equations cover a variety of cases—such as fully suspended lines, lines along the seabed, or slack lines—but none previously supported a sloped seabed. A new case has been added that considers a mooring line that lays partially on the seabed and with seabed slope in the plane of the mooring line's profile.

2.1.1 Catenary Equations for a Sloped Seabed.
Compared to the common case of a catenary mooring line partially laying along a flat seabed, the case of a sloped seabed introduces two fundamental changes. First, the touchdown point on the seabed is no longer defined by having a zero vertical tension component but instead has a tension vector parallel to the seabed slope. Second, the sloped seabed causes a tension variation across the line length on the seabed due to the angled normal force.

Figure 1 shows the general configuration and labeling conventions used in this work, where A indicates the anchor point, B indicates the platform connection point, and T indicates the touchdown point.

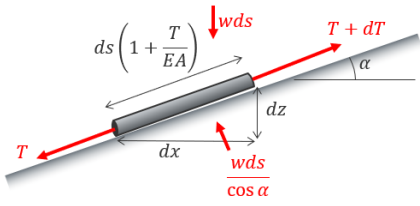
FIGURE 1: CATENARY MOORING LINE PROFILE ON A SLOPED SEABED

Figure 2 shows the forces on an small element of a mooring line laying along a sloped seabed. The tension gradient along the seabed is:

$$\frac{dT}{ds} = w \sin \alpha + w c_b, \qquad (1)$$

where w is the line's weight per unit length, T is tension, s is length coordinate, and c_b is seabed friction coefficient. Although

FIGURE 2: DIFFERENTIAL ELEMENT OF A MOORING LINE ON A SLOPED SEABED

seabed friction is not a main feature of the model presented here, we include it in the formulation for completeness.

We denote the total unstretched line length L and the portion of it laying along the seabed L_b. The location of the touchdown point, T, can be found by considering the forces at that point. The tension at the touchdown point can be calculated based on L_b and an assumed anchor tension, T_A, as

$$T(s = L_B) = T_A + w(\sin\alpha + c_b)L_b. \qquad (2)$$

This approach assumes the stiffness and slope are small enough that the line tension never reaches zero. For convenience, we use H and V to denote the horizontal and vertical components of line tension along the line. For the portion along the seabed, the line slope is $alpha$, such that

$$H_T = H_A + w(\sin\alpha + c_b)L_b\cos\alpha, \qquad (3)$$

$$V_T = V_A + w(\sin\alpha + c_b)L_b\sin\alpha. \qquad (4)$$

We can also relate the tension components at the touchdown point to those at end B using the assumptions that the only difference in forces arises from the suspended weight of the line, resulting in

$$H_T = H_B, \qquad (5)$$

$$V_T = V_B - w(L - L_b). \qquad (6)$$

Rearranging (3) for T_A and substituting into (4) results in some terms canceling out to yield

$$H_B\tan\alpha = V_B - w(L - L_b), \qquad (7)$$

which gives an expression for the laid length:

$$L_b = L - \frac{V_B - H_B\tan\alpha}{w}. \qquad (8)$$

Next, we can calculate the stretched positions and the tensions of the line along the seabed and then through the water column.

For the portion along the seabed, the stretched length is found by integrating the strain over the unstretchend length:

$$L(s) = \int_0^s 1 + \frac{T(s)}{EA}ds = s + \frac{T_As}{EA} + \frac{w(\sin\alpha + c_b)s^2}{2EA} \qquad (9)$$

The x and y coordinates of the touchdown point can then be found:

$$x_T = \left(L_b + \frac{T_AL_b}{EA} + \frac{w(\sin\alpha + c_b)L_b^2}{2EA}\right)\cos\alpha, \qquad (10)$$

$$z_T = \left(L_b + \frac{T_AL_b}{EA} + \frac{w(\sin\alpha + c_b)L_b^2}{2EA}\right)\sin\alpha. \qquad (11)$$

Now that the touchdown point is known, the regular catenary equations can be used to compute the profile and tensions of the suspended portion of the line:

$$x_B - x_T = \frac{H_f}{w}\left[\sinh^{-1}\left(\frac{V_T + wL_s}{H_f}\right) - \sinh^{-1}\left(\frac{V_T}{H_f}\right) + \frac{H_f L_s}{EA}\right] \qquad (12)$$

$$z_B - z_T = \frac{H_f}{w}\left[\sqrt{1 + \left(\frac{V_T + wL_s}{H_f}\right)^2} - \sqrt{1 + \left(\frac{V_T}{H_f}\right)^2} + \frac{2V_T L_s + wL_s^2}{2EA}\right] \qquad (13)$$

where $L_s = L - L_{bot}$ is the suspended length of the line.

These two equations follow the familiar form of catenary equations, with two knowns (the x and y distances) expressed as nonlinear functions of two unknowns (the horizontal and vertical tensions at End B). Solving these catenary equations with a sloped seabed follows just a slightly modified solution sequence compared to those for a flat seabed because the touchdown location also needs to be computed. The iterative process implemented in MoorPy is as follows:

1. Input known x_B and z_B distances, seabed slope α, and initial guesses for H_B and V_B

2. Calculate L_b from (8)

3. Calculate the touchdown point location, considering stretch along the seabed from (10-11)

4. Calculate the predicted x_B and z_B distances from (12-13)

5. Compute the error in the x_B and z_B calculations, adjust the H_B and V_B guesses accordingly, and iterate.

In MoorPy, the iterative process is handled by a Newton's method solver using analytic derivatives.

2.1.2 Three-Dimensional Seabed Surfaces. The two-dimensional implementation through the catenary equations is applied to a three-dimensional scenario using a heading rotation. The slope is taken to only be the seabed slope component along the line's heading direction. Any slope in the out-of-plane direction is neglected, keeping a straight line along the seabed and neglecting any side force from seabed contact. This is equivalent to assuming that seabed friction would prevent a mooring line from slipping laterally down a seabed slope.

To support realistic nonuniform seabed bathymetries, we implemented a surface mesh to describe the seabed depth at points over a rectangular x-y grid. Any list of x and y coordinates can be provided, along with the two-dimensional array of depths over those grid points. The MoorPy model interpolates over this surface grid to determine the local seabed depth beneath any part of the mooring system.

We use a bilinear interpolation scheme, following the same approach as in MoorDyn, for which more information can be

3

found in [4]. For any mooring line with seabed contact at one end, corresponding to an anchored line section, the seabed slope is computed at the anchor end based on the slope of the panel in which it falls. The projection of this slope in the vertical plane of the mooring line is then taken and used in the catenary calculations described above.

The slope of the seabed beneath the mooring line in three dimensions is defined by the unit normal vector $\hat{n}$.

$$\hat{n} = \text{unit}\left(\left\{\begin{array}{c} \frac{\partial z}{\partial x} \\ \frac{\partial z}{\partial y} \\ 1 \end{array}\right\}\right), \tag{14}$$

where the partial derivatives represent the seabed slope in each direction, found through a bilinear interpolation.

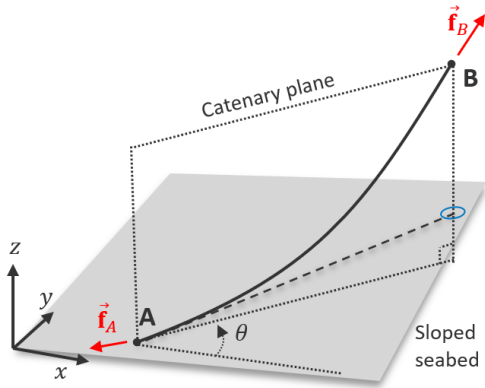We define vector $\mathbf{d}$ to be the displacement vector from End A to End B:

$$\mathbf{d} = \mathbf{r}_B - \mathbf{r}_A, \tag{15}$$

where $\mathbf{r}$ denotes a global x/y/z coordinates vector.

The line heading in the horizontal plane is defined as

$$\theta = \tan^{-1}\frac{a_2}{a_1}. \tag{16}$$

We can then create a rotation matrix that will apply a rotation of $-\theta$ about the z axis to rotate the mooring line's profile to lie along the x-z plane, as illustrated in Figure 3.

FIGURE 3: MOORING LINE IN A VERTICAL PLANE ON A SLOPED SEABED

The required rotation matrix is:

$$\mathbf{R} = \begin{bmatrix} \cos\theta & \sin\theta & 0 \\ -\sin\theta & \cos\theta & 0 \\ 0 & 0 & 1 \end{bmatrix}. \tag{17}$$

To account for the seabed slope, we apply this rotation to the seabed unit normal vector to find the seabed normal vector in the rotated reference frame:

$$\hat{n}' = \mathbf{R}\hat{n}, \tag{18}$$

where the prime accent denotes that the quantity has undergone a rotational transformation.

The seabed slope in the plane of the mooring line can then be found according to

$$\frac{\partial z'}{\partial x'} = \frac{-\hat{n}'_1}{\hat{n}'_3}. \tag{19}$$

The incline angle experienced by the mooring line is then

$$\alpha = \tan^{-1}\left(\frac{\partial z'}{\partial x'}\right). \tag{20}$$

Following this approach and the sloped-seabed catenary process described previously, mooring line profiles on a three-dimensional bathymetry grid can be calculated, provided that the line does not lay across multiple grid panels, which is a capability for future work. The above equations for rotation and slope may seem to have unnecessary steps, but the formulation is made general so that it can also be used for rotational transformations that allow modeling of current loads, described next.

2.2 Current Drag Loads on Mooring Lines

To account for current drag loads on mooring lines and dynamic cables, we formulate an approach that uses rotated reference frames. The total current drag force on a mooring line or cable section is computed based on local current velocities and directional drag coefficients. We make the approximation that the resulting line profile will fall in a plane that is no longer necessarily aligned with the gravity vector (vertical) but is instead aligned with the vector sum of the total weight and drag force on the line. We apply the catenary equations in the rotated reference frame, replacing the usual weight term with a weight-plus-drag term, and then account for any change in the in-plane seabed slope due to the rotational transformation.

The formulation for current drag forces is fully three-dimensional in supporting current in any direction relative to the mooring line profile. As before, we define coordinates relative to End A of the mooring line in the inertial orientation frame (z is up, and the line may be in any heading in the x-y plane). A unit vector point from End A to End B is denoted $\hat{a}$.

To calculated the current drag force, we discretize the mooring line into n segments between $n+1$ nodes. At each node, i, we compute drag forces due to adjacent half-segments considering the tangent direction of the node, $\hat{q}_i$, using the same approach as done in the dynamic lumped-mass model MoorDyn [14]. The sum of all current drag force vectors across the nodes of a mooring line is denoted $\mathbf{f}_c$

To explain the application of the current drag force, we first note that the usual weight per unit length (w_0) used in the catenary calculations can be expressed as a vector quantity:

$$\mathbf{w}_0 = \left\{\begin{array}{c} 0 \\ 0 \\ -w_0 \end{array}\right\}. \tag{21}$$

The first step of the current drag implementation is to add the drag force per unit length to $\mathbf{w}_0$ to obtain a combined force-per-unit-length vector:

$$\mathbf{w} = \mathbf{w}_0 + \frac{\mathbf{f}_c}{L}. \tag{22}$$

4

This equation assumes that the current drag force can be approximated as evenly distributed over the length of the line. Insofar as this approximation is suitable, a catenary solution with this combined force vector will yield mooring line profiles and tensions that account for the current drag force.

To apply the two-dimensional catenary equations, we need to identify the orientation of the catenary, which may no longer be vertical. Figure 4 illustrates how the catenary plane is affected by the direction of $\mathbf{w}$. For generality, the seabed is also shown to have a slope.
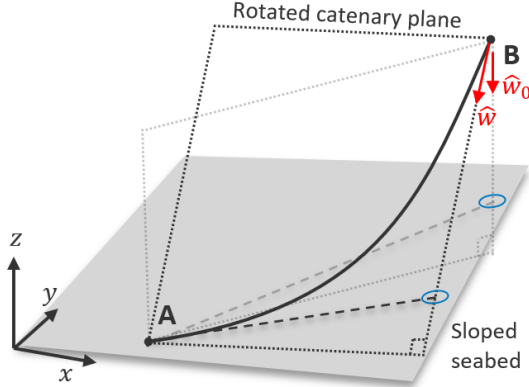
FIGURE 4: INCLINED CATENARY PLANE DUE TO CURRENT DRAG FORCE

We determine the catenary plane orientation in two steps. First, we calculate a rotation matrix using the Rodriguez rotation formula that will rotate the vertical downward unit vector, $\hat{\mathbf{w}}_0$, to align with the new external force vector, $\hat{\mathbf{w}}$. This rotation matrix is

$$
\mathbf{R}_w = \begin{bmatrix} 1 & -t_3 & t_2 \\ t_3 & 1 & -t_1 \\ -t_2 & t_1 & 1 \end{bmatrix} + \begin{bmatrix} 0 & -t_3 & t_2 \\ t_3 & 0 & -t_1 \\ -t_2 & t_1 & 0 \end{bmatrix}^2 \left(\frac{1 - \hat{\mathbf{w}} \cdot \hat{\mathbf{w}}_0}{|\hat{t}|^2} \right),
$$
(23)

where

$$
\mathbf{t} = \hat{\mathbf{w}}_0 \times \hat{\mathbf{w}}.
$$
(24)

Next, we compute the heading in the rotated reference frame by using (16), but considering the already rotated orientation of the line:

$$
\theta' = tan^{-1} \frac{d_2'}{d_1'},
$$
(25)

where $\mathbf{d}' = \mathbf{R}_w \mathbf{d}$.

Similarly as in (17), a new rotation matrix about z' can be applied that will rotate $\mathbf{d}'$ onto the x-z plane. We denote this rotation matrix $\mathbf{R}_\theta$. Combining with $\mathbf{R}_w$ gives a single rotation matrix, $\mathbf{R}$ that will transform from the line's original three-dimensional orientation to an orientation in which the line profile falls on the x-z plane:

$$
\mathbf{R} = \mathbf{R}_\theta \mathbf{R}_w.
$$
(26)

Having found this rotation matrix, we can use it in the same way as shown previously for a sloped seabed. This includes

computing the new seabed normal vector relative to the plane of the catenary and then finding the in-plane seabed slope using (18-20). Crucially, this approach includes both the effect of an originally sloped seabed, as well as the additional effective slope that is seen in the plane of the catenary by virtue of the non-vertical direction of the external force vector $\mathbf{w}$.

With this rotational transformation, the catenary equations described in Section 2.1 can be applied to calculate the line profile and tensions in response to weight, current force, and seabed slope. This calculation uses the transformed horizontal and vertical distances from d', the transformed seabed slope, α', and the altered external force vector magnitude, w. Once the catenary results are computed, they can be transformed back to the original three-dimensional reference frame by applying the inverse (or transpose) of the rotation matrix $\mathbf{R}$.

Altogether, this transformation approach results in mooring line or cable profiles that are responsive to the distributed current drag load. The implementation for modeling seabed slopes mentioned previously allows for seabed contact to be properly modeled, even when including the effects of current.

2.3 Current Drag Loads on Floating Substructures

When modeling a floating wind array's equilibrium positions and forces, the current drag forces on the floating substructures can be a significant contributor. To account for these drag loads, the static force calculation routines in RAFT have been expanded to include a full Morison equation calculation of steady drag forces in response to a user-specified current profile.

RAFT models the substructure as a combination of linear members with round or rectangular cross sections. These members have many parameters, including cross-sectional properties and hydrodynamic coefficients at various station points along the member length. To calculate hydrodynamic loads, the member is discretized along its lengths into short segments, over which a strip-theory hydrodynamic approach is applied using Morison's equation.

For computing the current drag force, each strip of a member has a drag coefficient interpolated from input drag coefficients at specified locations along the length of the member. Similarly, the diameter (or width for rectangular members) is interpolated to calculate the frontal area of the strip over which the drag force should be calculated.

For each member strip, a local current velocity is calculated based on that strip's node position and orientation. This velocity, along with the strip's area and drag coefficient, is used to calculate the total drag force on that strip. The local current velocity is interpolated from a user-input velocity profile, allowing the segment's drag force to then be calculated. The current velocity can be uniform or modeled as a standard power-law profile. In the current work, we demonstrate with a uniform current profile.

Drag forces on member ends are also computed. Summing these forces up produces a total current drag force on the substructure.

3. RESULTS

The new capabilities are verified by comparing results with those from MoorDyn and OrcaFlex in equivalent steady-state

5

scenarios.

The general scenario being considered is a floating spar with three semi-taut mooring lines. The mooring system properties are listed in Table 1, and the sectional mooring line properties are listed in Table 2.

TABLE 1: MOORING SYSTEM CONFIGURATION

Property	Value
Number of lines	3
Water depth (m)	400
Anchoring radius (m)	400
Fairlead radius (m)	10
Fairlead depth (m)	30
Section 1 type	Chain
Section 1 unstretched length (m)	440
Section 2 type	Rope
Section 2 unstretched length (m)	460

TABLE 2: MOORING LINE TYPE SECTION PROPERTIES

Name	Chain	Rope
Volume-equivalent diameter (m)	0.3179	0.1412
Linear mass (kg/m)	620.8	21.50
Stiffness coefficient, EA (MN)	2664	192
Transverse drag coefficient	1.2	1.2
Axial drag coefficient	0.2	0.2

The floating platform is simplified to be a single cylinder of 85 m draft and 19 m diameter. Its mass is set as 24,270 metric tonnes, centered at 56.37 m below the waterline. These properties, described in Table 3 are chosen to roughly support the IEA 15-MW reference wind turbine [15].

TABLE 3: FLOATING SUBSTRUCTURE PROPERTIES

| Property	Value
Draft (m)	85
Diameter (m)	19
Displacement (m^3)	24100
Mass (t)	24,270
Center of mass depth (m)	56.37

3.1 Mooring Line Sloped Seabed Case

This case considers the mooring system undisplaced profiles over a seabed slope of 10% in the y direction. For simplicity, the mooring system design is not adapted to the seabed slope. Rather, the anchor points are just assumed to be on the (now-sloped) seabed at the original x and y coordinates. The fairlead ends are held constant, and the mooring lines are allowed to settle into equilibrium. Both MoorPy and MoorDyn are used in this case to provide a point of comparison. Figure 5 shows a comparison of the mooring line profiles from both models in this scenario.
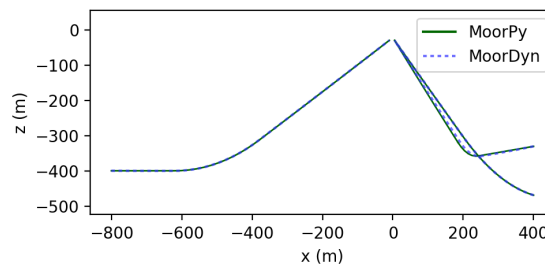
The results show good agreement between the models. All mooring lines follow the seabed slope, and the vertical profiles of the three lines all have close agreement between models. The one
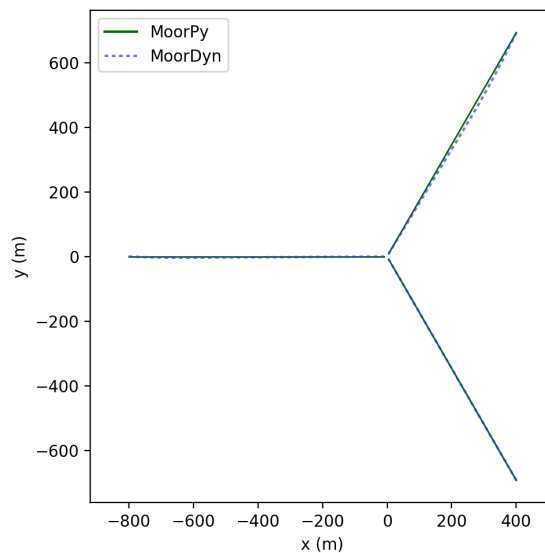
(a) Top view
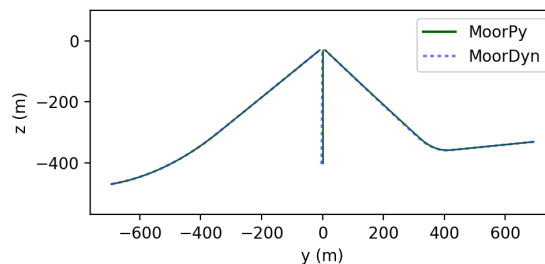
(b) Front view

(c) Side view

FIGURE 5: MOORING PROFILES WITH 10% SEABED SLOPE IN Y

notable difference is in the top view of the mooring line that travels uphill to its anchor point. MoorPy predicts a straight trajectory for this line, as assumed by the planar approach, whereas MoorDyn predicts a curved path along the sloped seabed.

3.2 Mooring Line Current Loads Case

This case considers the effect of current drag forces on the mooring lines with a level seabed. Similar to the previous case, MoorPy and MoorDyn models are run with the fairlead points held fixed, and the equilibrium profiles of the mooring lines are compared. Because the presence of current disrupts the mooring lines from their normal vertical profiles, the results are presented in terms of both the undisplaced and displaced results

from MoorPy and then the displaced results from MoorDyn for comparison.
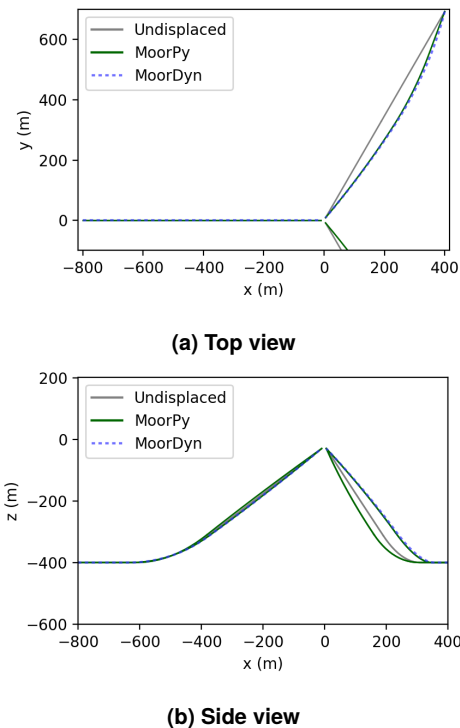

(a) Top view

(b) Side view

FIGURE 6: MOORING PROFILES WITH 3 M/S CURRENT IN X

Figure 6 shows the results for a current of 3 m/s in the x direction. Here, a small in-plane change is visible in the profile of the line that runs parallel to the current direction. The lines that run at an angle to the current direction show displacements both in-plane and out of plane.

Figure 7 shows the results for a current of 3 m/s in the y direction. Out-of-plane deformations of the line profile for the line perpendicular to the current are visible, as well as deformations both in and out of plane for the lines that run at an angle to the current direction.

In general, these results with current show the expected effects of current on the mooring line profiles. They also show very good agreement between MoorDyn and MoorPy, suggesting that, for these scenarios, the approach to current drag in MoorPy works reasonably well.

3.3 Combined Current Loads and Sloped Seabed Case

The current capability can also be applied to a sloped seabed. This case considers a 3 m/s current in the x direction and a seabed slope of 10% in the y direction—the same seabed condition as in Section 3.1.

To provide a further point of verification, this case is run with MoorPy, MoorDyn, and OrcaFlex. The profiles predicted by these models are shown in Figure 8. Table 4 compares the fairlead tensions in the three lines, as predicted by each model.

In general, the results between all three models show good agreement. Just as in Section 3.1, the mooring line that runs up the slope to the anchor is predicted to curve along the seabed by
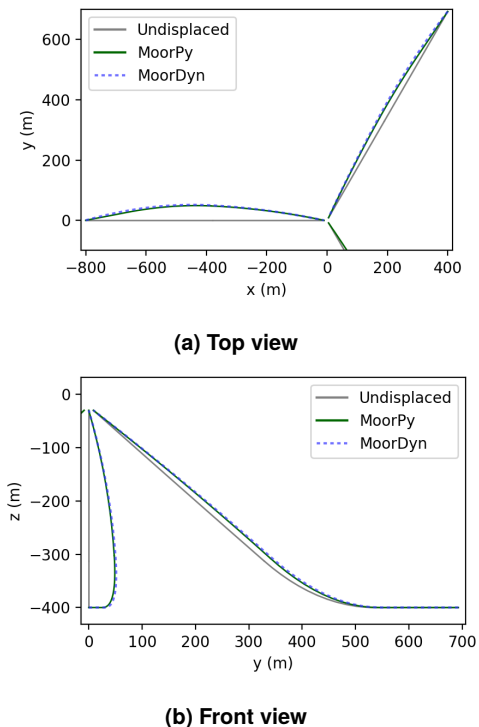

(a) Top view

(b) Front view

FIGURE 7: MOORING PROFILES WITH 3 M/S CURRENT IN Y

TABLE 4: LINE TENSION COMPARISON OF FIXED SYSTEM IN 3 M/S CURRENT IN X AND 10% SEABED SLOPE IN Y
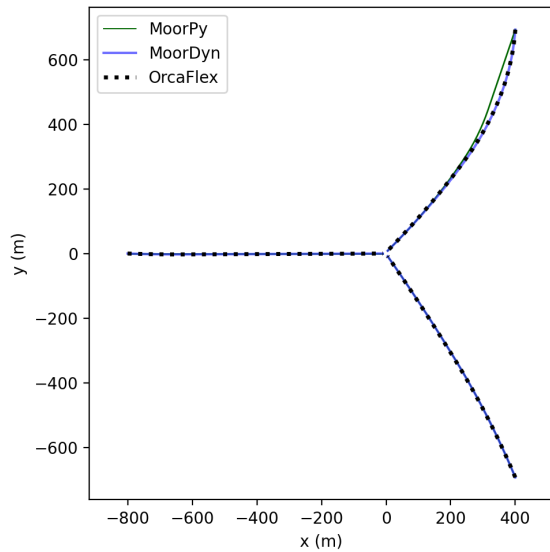
	OrcaFlex	MoorDyn	MoorPy
Line 1 Tension (kN)	1686	1652	1439
Line 2 Tension (kN)	2333	2323	2326
Line 3 Tension (kN)	5201	5190	5219

MoorDyn, but not by MoorPy. The OrcaFlex results are similar to MoorDyn in this regard, since both models consider current forces on the seabed nodes and seabed friction is not enabled to restrain the line motion along the seabed. In a separate simulation with seabed friction included in OrcaFlex, the line profiles along the seabed agreed closely with the MoorPy results, suggesting that the assumption in MoorPy of the line being straight along the seabed has a similar effect as including seabed friction. This nuance aside, the general agreement between all three models gives a reassuring verification of the MoorPy implementation.
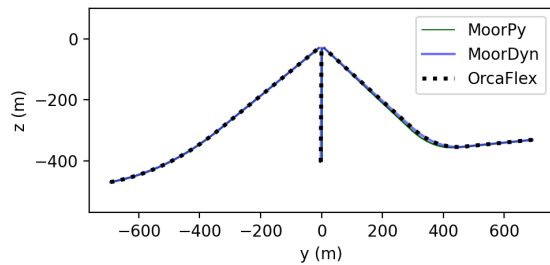
3.4 Current Loads on a Full Floating System

To check the effect of current on a full floating system, we include RAFT to model the floating platform that is attached to the mooring system modeled in MoorPy. This case considers a level seabed and uniform current at 3 m/s in the x direction through the height of the water column.
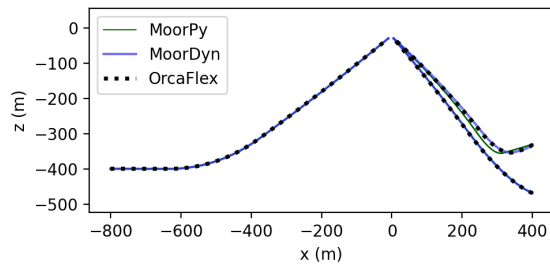
Before running this coupled floating simulation, we first checked that the current drag forces predicted on the floating cylinder were consistent. Applying the 3 m/s horizontal current to the cylindrical geometry described in Table 3, RAFT, MoorDyn, and OrcaFlex all predicted the same results to within 1%: a surge force of 662 kN and a moment as measured relative to the
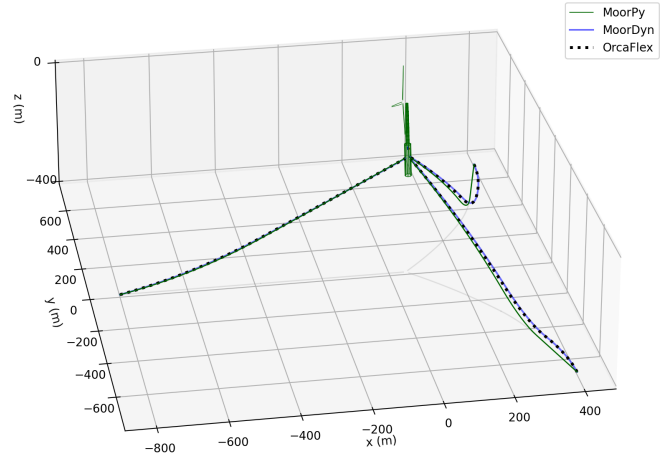
7

(a) Top view

(b) Front view

(c) Side view

FIGURE 8: MOORING PROFILES WITH 3 M/S CURRENT IN X AND 10% SEABED SLOPE IN Y

FIGURE 9: FLOATING SYSTEM OFFSETS WITH 3 M/S CURRENT

TABLE 5: LINE TENSION AND MEAN OFFSET COMPARISON OF FLOATING SYSTEM IN 3 M/S CURRENT
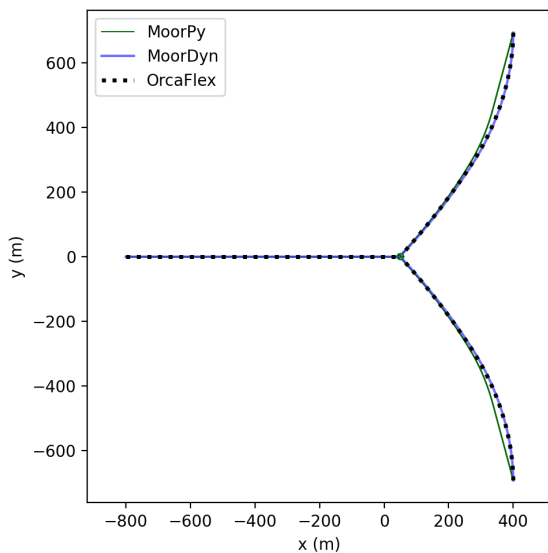
Model	OrcaFlex	MoorDyn	MoorPy
Line 1 Tension (kN)	1701	1785	1601
Line 2 Tension (kN)	8883	8954	8312
Line 3 Tension (kN)	1701	1785	1601
Surge (m)	52.4	51.6	49.3

mooring line profiles partway down the lines is much greater than the difference in platform offsets, as indicated by the line profiles being in close agreement near the fairleads. As already seen in Section 3.3, the MoorDyn and OrcaFlex results agree very closely, while the MoorPy results have slightly less out-of-plane deflection from the current, particularly along the seabed. In general, these results demonstrate that, for this scenario, the implementation in MoorPy and RAFT can reasonably predict the floating system offsets and mooring line profiles resulting from a steady current load.
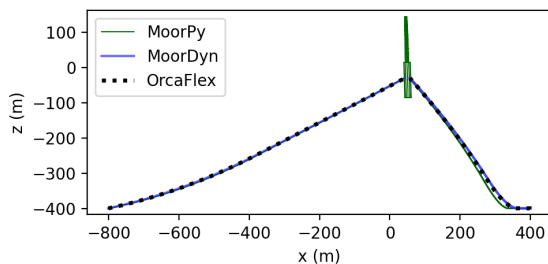
4. CONCLUSIONS

Capabilities for modeling the effects of seabed bathymetry and current drag loads on floating wind turbines are now available in the MoorPy and RAFT models. We derived catenary equations to model mooring lines on a sloped seabed and set up a method to support a three-dimensional bathymetry grid. To account for current drag loads on mooring lines, we derived and implemented a method that adds the current force to the weight force in the catenary equations and uses a rotational transformation to account for the change in force direction. This transformation also makes use of the seabed slope capability. By also including a mean current drag force on floating substructure members in RAFT, we provide a quasi-static capability for predicting the mean system response to current loads.

We demonstrate and verify this new capability through a set of cases involving seabed slope and uniform current fields. By comparing with results from MoorDyn and also OrcaFlex, we find good agreement in the predictions from the quasi-static model. The model has typical computation times of less than 1 second

waterline of 28 MN-m.

We then ran the models to simulate the floating system with the cylinder free to move, and found where each model predicted the system would settle into equilibrium. Figure 9 shows a three-dimensional comparison of the mooring line profiles predicted by all three models, including the offset floating platform position predicted by RAFT. Figure 10 provides two-dimensional views of the same. Table 5 compares the fairlead tensions and platform surge offsets predicted across the three models.

The results show good agreement in the up-current line (Line 2) profile, and similar modest levels of disagreement in the angled mooring lines, as seen in previous results. The difference in

8

(a) Top view

(b) Side view

FIGURE 10: FLOATING SYSTEM OFFSETS WITH 3 M/S CURRENT

for any of the cases presented here. As such, it represents a very efficient method to evaluate the effect of mean current loads on floating systems.

These model additions provide a step forward toward rapidly evaluating a floating wind array's response to environmental loads under realistic site conditions with currents and sloped seabeds. Future work will consider adapting these techniques to scenarios with nonuniform currents and seabed slope changes over the length of a mooring line.

ACKNOWLEDGMENTS

REFERENCES

[1] P. Stanton, D. Tidwell, and J. Lloyd, "Sloping Sea Floors," *Proceedings of OTC Offshore Technology Conference*, pp. OTC–1158–MS, 04 1970.

[2] S. Viswanathan and C. Holden, *Modelica Component Models for Non-diffracting Floating Objects and Quasi-static Catenary Moorings*. Liu Electronic Press, 2020.

[3] A. Feng, H. S. Kang, B. Zhao, and Z. Jiang, "Two-Dimensional numerical modelling of a moored floating body under sloping seabed conditions," *Journal of Marine Science and Engineering*, vol. 8, p. 389, June 2020.

[4] S. Housner, E. Lozon, B. Martin, D. Brefort, and M. Hall, "Seabed bathymetry and friction modeling in MoorDyn," *Journal of Physics: Conference Series*, 2022.

[5] P. Desiré, Álvaro Rodríguez-Luis, and R. Guanche, "Simulation of mooring lines in complex bathymetries using a finite element method," *Ocean Engineering*, vol. 272, p. 113827, 2023.

[6] S. Roy and A. K. Banik, "Dynamic responses of an FPSO moored on sloped seabed under the action of environmental loads," *Ocean Systems Engineering*, vol. 8, pp. 329–343, Sept. 2018. Number: 3.

[7] M. Batista and M. Perkovič, "Computation of mooring chain with the touchdown on an inclined seabed," *Journal of Marine Engineering & Technology*, vol. 21, no. 1, pp. 9–22, 2022.

[8] J. M. Jonkman, *Dynamics Modeling and Loads Analysis of an Offshore Floating Wind Turbine*. PhD thesis, University of Colorado at Boulder, 2007.

[9] M. Masciola, J. Jonkman, and A. Robertson, "Implementation of a multisegmented, Quasi-Static cable model," OnePetro, June 2013.

[10] Y. T. Chai, K. S. Varyani, and N. D. P. Barltrop, "Semi-analytical quasi-static formulation for three-dimensional partially grounded mooring system problems," *Ocean Engineering*, vol. 29, pp. 627–649, June 2002.

[11] P. Trubat, C. Molins, and X. Gironella, "Quasi-dynamic mooring line model," *Ocean Engineering*, vol. 243, p. 110133, 2022.

[12] M. Hall, S. Housner, D. Zalkind, P. Bortolotti, D. Ogden, and G. Barter, "An Open-Source Frequency-Domain model for floating wind turbine design optimization," *Journal of Physics: Conference Series*, vol. 2265, p. 042020, May 2022.

[13] M. Hall, S. Housner, S. Sirnivas, and S. Wilson, "Moorpy (quasi-static mooring analysis in python)," jul 2021.

[14] M. Hall and A. Goupee, "Validation of a lumped-mass mooring line model with DeepCwind semisubmersible model test data," *Ocean Engineering*, vol. 104, pp. 590–603, Aug. 2015.

[15] E. Gaertner, J. Rinker, L. Sethuraman, F. Zahle, B. Anderson, G. Barter, N. Abbas, F. Meng, P. Bortolotti, W. Skrzypinski, G. Scott, R. Feil, H. Bredmose, K. Dykes, M. Shields, C. Allen, and A. Viselli, "Definition of the IEA 15-Megawatt offshore reference wind turbine," report, National Renewable Energy Laboratory, 2020.